Research Article | Vol. 29, No. 17 / 16 August 2021 / Optics Express 26553
Optics EXPRESS

Bayesian approach for developing threshold color-difference models by the strip-pair comparison method

FERNANDO BRUSOLA,* IGNACIO TORTAJADA, BEGOÑA JORDÁ, JIMENA GONZÁLEZ-DEL RÍO, AND ISMAEL LENGUA

Centro de Investigación en Tecnologías Gráficas, Universitat Politècnica de València, Camino de Vera s/n, 46022 Valencia, Spain
fbrusola@upv.es

Abstract: A Bayesian approach alternative to the one used in the strip-pair comparison method for developing threshold color-difference models is presented in this paper. Strip-pair comparison method is based on the construction of color-control strips made of pairs of patches put in contact and ordered by increasing the CIELAB color difference. Observers are required to indicate the number of the pair of patches in every strip for which they begin to perceive a just noticeable color difference. Frequency data obtained, from repeating several times the visual assessment, is recorded to build a Bayesian multinomial logistic regression model, which allows the determination of the coefficients of the color discrimination ellipsoids. The results of the Bayesian approach agree closely with the results obtained to validate strip-pair comparison method for the same theoretical frequency data. The main advantage of the Bayesian approach over many other methods is that it allows a direct analysis of the statistical variability of the estimated parameters by means of confidence intervals and other measures of statistical variability.

1. Introduction

Scientific progress in defining and configuring new color difference models has been made possible by the increase and improvement of datasets. Among the many datasets published by the authors, the BFD [1,2], RIT-Dupont [3], Leeds [4] and Witt [5] datasets have been used to develop several color difference formulas under standard conditions [6], as CIEDE2000, recommended by ISO/CIE [7] for industrial applications. For the development of color difference models based on color appearance models (CAM), such as CIECAM02 [8] and CAM16 [9], other datasets [10–17] were developed to improve and evaluate the models. Lately, Xu et al. [18] have generated a new dataset in order to verify the performance of different color difference models for HDR images reproduction. Improved color reproduction technology in new media will make it necessary to increase and improve the quality of new color difference datasets, following the CIE guidelines [19–21] on maintaining a coordinated effort for the evaluation of color differences.

Most commonly used methods to generate color difference datasets have been the grayscale method (GSM) [22,23] and the pair comparison method (PCM) [3,24,25]. Recently, Brusola et al. [26] have proposed the strip-pair comparison method (SCM), based on the serial exploration method proposed by Torgerson [27], to evaluate color differences at threshold as an alternative to GSM and PCM to accelerate data collection.

SCM has been tested by Brusola et al. [28] to evaluate parametric effects of its use with respect to PCM for color differences around CIE red color center at threshold for pairs of color samples in contact, separated by a 0.5 mm black line and spaced 3 mm apart on a white background. The results led to the conclusion that SCM has very little effect on the shape and orientation of the color discrimination ellipses when pairs of patches are separated by a 0.5 mm black line or separated 3 mm apart on a white background. The size of the ellipses tended to be larger

#432157 https://doi.org/10.1364/OE.432157
Journal © 2021 Received 21 May 2021; revised 26 Jul 2021; accepted 26 Jul 2021; published 3 Aug 2021

Optics EXPRESS

for SCM than for PCM, although the size obtained by SCM agreed more closely with the size reported by other authors for the CIE red color center [16,29].

Brusola et al. [30] proposed a Bayesian alternative for the construction of PCM-based color difference models. This approach was validated with simulated theoretical data and with real data published by Witt & Döring [31] for the CIE green color center. Among other advantages over many other methods, the Bayesian approach allows to evaluate the uncertainty of the estimated model parameters directly in terms of probability [32,33], using confidence intervals or other measures of statistical variability, and, in general, results are easier to interpret than by the frequentist approach. The subtleties involved in the correct use and interpretation of p-values and significance levels in hypothesis testing in classical inference statistics (frequentist) have been debated at length in the last decade and have forced the specialists to publish a series of guidelines on what to do and what not to do when reporting research results [34]. Many controversies have arisen in the past about the advantages and disadvantages of using the frequentist versus Bayesian approach, and although the divide persists, there seems to be a consensus on using the insights from both schools to solve complex problems [35]. As a result, a set of new guidelines on how to analyze statistical evidence from data has been proposed [36].

In the current era, the use of Bayesian methods has experienced great growth in the fields of genetics, artificial intelligence and medicine. And it is very likely that their use will extend to other fields of knowledge, including the construction of color difference models. This paper is intended as a small contribution to this and proposes a methodology to perform SCM by the Bayesian approach and the determination of the parametric effects, due to its application, with respect to conventional SCM.

2. Method

The SCM [26] is based on the construction of strips of patches organized by rows and columns. In one dimension (row or column) of the strip the patches are arranged in pairs and in the other dimension one of the patches of the pair should be kept colorimetrically constant while the other should vary so that the color difference with respect to the constant patch increases in regular steps, up to a maximum difference in the last pair of patches. Such strips are constructed so that the color difference varies according to different vector directions in the *CIELAB* color space around a selected color center. In Fig. 1 is shown an example of a strip, consisting of 10 pairs of patches, for the CIE gray color center ($L^* = 62,\ a^* = 0, b^* = 0$) in the unitary vector direction ($dL^* = 1, da^* = 0, db^* = 0$), with a minimum intended color difference ΔE^*_{ab}=0 in patch *#1*, a maximum intended difference ΔE^*_{ab}=4 in patch *#10* and with intended color differences in the intermediate patches with regular increments of color difference ΔE^*_{ab}=4/9. The rest of the strips around the selected color center would be constructed similarly according to the unit vector belonging to the chosen set of directions. The set of 26 vector directions selected in [26] corresponds to the set of directions in CIELAB space defined by the color center and vertices, the midpoint of the edges and the midpoint of the faces of a cube whose center coincides with the color center.

Observers will be asked to indicate the number of the pair of patches in each strip in which they observe the first just noticeable color difference (*JND*), assuming that in the patches before the selected one no color difference should be perceived. Thus, according to this method, only one record per strip will be recorded for every observation.

2.1. Bayesian statistical model

Our proposed Bayesian statistical model exhibits significant differences compared with that reported by Brusola et al. [30]. In the present study, the observed frequencies collected from the observers for each strip correspond to the outputs of a multinomial distribution. The probability for each pair to be selected in a strip should be proportional to the corresponding value from

Optics EXPRESS

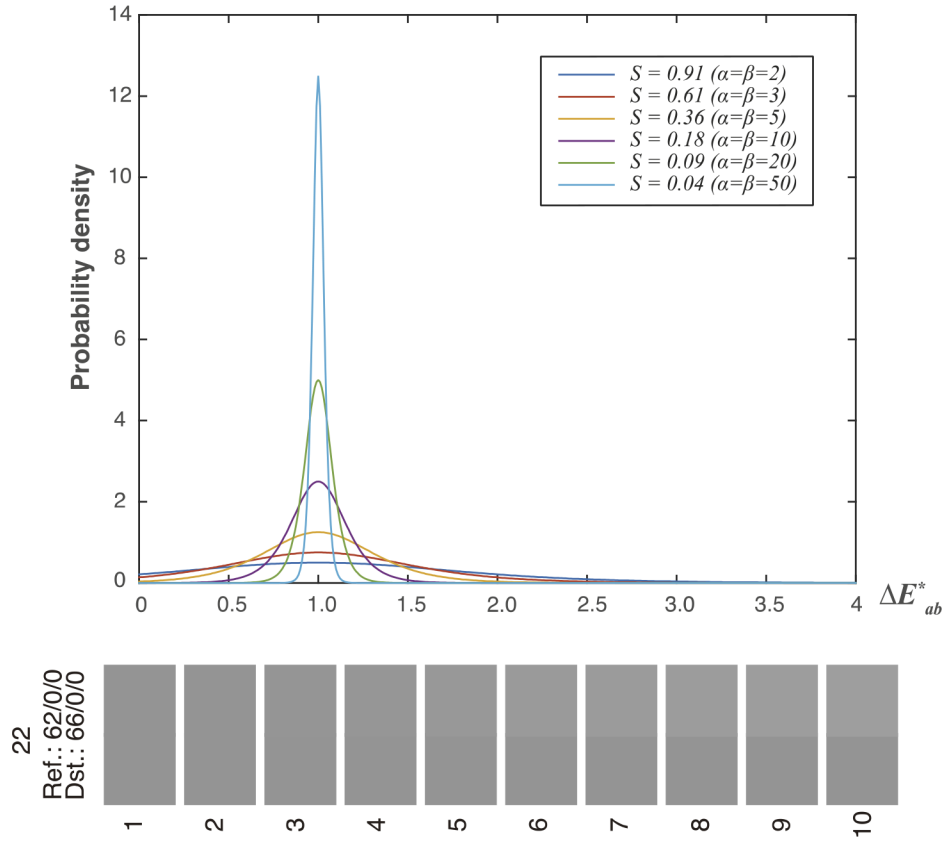

Fig. 1. The probability of selecting a pair of patches in a strip as the first pair whose color difference is just noticeable (*JND*) should be proportional to the values of a probability density function associated with the direction of the strip. The pair of patches nearer to the median above the 50% cumulative probability point should be the most probable *JND* pair.

the probability density distribution (*pdf*) of the median of the psychometric function. Different probability density functions are shown in Fig. 1 for the logistic psychometric function and different parameters α=β. The logistic probability density function corresponds to the derivative of the logistic function $p = 1/(1 + e^{(\alpha-\beta\Delta E)})$.

In our proposed model, the observed selection frequency for each pair of patches in a strip follows a multinomial distribution, as stated by Eq. (1).

$$\vec{r}_i = [r_{i1} \ldots r_{ik} \ldots \ r_{iK} \ ] \sim Multinomial(nRep, \vec{p}_i) \tag{1}$$

where r_{ik} is the number of times the k^{th} couple of patches is selected by observers in strip i after *nRep* repetitions, and p_{ik} is the probability of selecting the k^{th} patch pair from strip i. Note that $\sum_{k=1}^{K} p_{ik} = 1$, where K is the number of patch pairs in a strip. Then the probability distribution function (*pdf*) for the r_{ik}, k=1... K, values in each strip i would be given by Eq. (2).

$$f(\vec{r}_i|n, \vec{p}_i) = \frac{n!}{r_{i1}! \ldots \ r_{iK}!} p_{i1}^{r_{i1}} \ \ldots \ p_{iK}^{r_{iK}}, \ n = nRep \tag{2}$$

Optics EXPRESS

The estimated values p_{ik} (probability of selecting pair patch k in strip i) is determined according to Eq. (3), which ensures $\sum_{k=1}^{K} p_{ik} = 1$.

$$p_{ik} = \frac{pd_{ik}}{\sum_{k=1}^{K} pd_{ik}} \tag{3}$$

where pd_{ik}, are the corresponding values of pdf of the median on each strip i, given by Eq. (4) for the color difference in every pair of patches given by Eq. (5).

$$pd_{ik} = pdf(\Delta E_{ik}) \tag{4}$$

$$\Delta E_{ik}^2 = g_1\Delta a_{ik}^2 + g_2\Delta b_{ik}^2 + g_3\Delta L_{ik}^2 + 2g_4\Delta a_{ik}\Delta b_{ik} + 2g_5\Delta a_{ik}\Delta L_{ik} + 2g_6\Delta b_{ik}\Delta L_{ik} \tag{5}$$

If we use as pdf the logistic probability distribution, the values of the density function for each pair of patches, ik, is given by Eq. (6).

$$pd_{ik} = \frac{\beta e^{(\alpha-\beta\Delta E_{ik})}}{(1+e^{(\alpha-\beta\Delta E_{ik})})^2} \tag{6}$$

The likelihood of the model parameters $\boldsymbol{g} = \{g_j | j = 1:6\}$ given the data $\boldsymbol{r} = \{r_{ik} | i = 1:nStrips,\ k = 1:K\}$, where r_{ik} are the observed frequencies, is the probability to observe the data $\boldsymbol{r}$ assuming that $\boldsymbol{g}$ are the model parameters and is given by Eq. (7).

$$L(\boldsymbol{g}|\boldsymbol{r}) = P(\boldsymbol{r}|\boldsymbol{g}) = \prod_{i=1}^{nStrips} multinomial\_pdf(r_{ik}, p_{ik}) \tag{7}$$

Once the data is observed and according to Bayes' rule, the posterior probability of the model shall be proportional to the product of likelihood by the prior probability of the parameters, given by Eq. (8).

$$P(\boldsymbol{g}|\boldsymbol{r}) \propto P(\boldsymbol{r}|\boldsymbol{g}) \prod_{j}^{6} P_j(g_j) = \prod_{i=1}^{nStrips} multinomial\_pdf(r_{ik}, p_{ik}) \prod_{j=1}^{6} P_j(g_j) \tag{8}$$

where $P_j(g_j)$ are the probability priors of the ellipsoid parameters g_j, $j = 1:6$.

If we use the *pdf* shown in Eq. (6), for the logistic case, and assume that $\alpha = \beta$, we must add a new factor, to include the prior probability of the independent coefficient α (see Brusola et al. [30]), as shown in Eq. (9). Note that setting $\alpha = \beta$ does not cause the problem to lose generality, because in Eq. (6), when ΔE_{ik} is substituted for Eq. (5), as $\beta = \alpha(\beta/\alpha)$ the constant (β/α) can be merged in coefficients g_j as a new coefficient $g_j' = (\beta/\alpha)^2 g_j$. So, if $\alpha = \beta$ in Eq. (6) then g_j parameters obtained by the Bayesian model would be the coefficients of the 50% probability color discrimination ellipsoid.

$$P(\boldsymbol{\Theta}|\boldsymbol{r}) \propto P_7(\alpha) \prod_{i=1}^{nStrips} multinomial\_pdf(r_{ik}, p_{ik}) \prod_{j=1}^{6} P_j(g_j) \tag{9}$$

where $\boldsymbol{\Theta} = \{g_j, \alpha | j = 1:6\}$, to include α in the model parameter set**.**

To ensure that Eq. (5) yield positive values, we use the Cholesky decomposition, similar to that in [30]. According to this decomposition, the matrix obtained as the product of a lower triangular matrix and its transpose is positive definite if all the diagonal elements of the triangular matrix are positive.

Optics EXPRESS

As stated previously, the coefficients g_j in Eq. (5) can be replaced with d_j according to the transformation expressed in Eqs. (10,11).

$$G = \begin{bmatrix} g_1 & g_4 & g_5 \\ g_4 & g_2 & g_6 \\ g_5 & g_6 & g_3 \end{bmatrix} = \begin{bmatrix} d_1 & 0 & 0 \\ d_4 & d_2 & 0 \\ d_5 & d_6 & d_3 \end{bmatrix} \begin{bmatrix} d_1 & d_4 & d_5 \\ 0 & d_2 & d_6 \\ 0 & 0 & d_3 \end{bmatrix} \tag{10}$$

$$G = \begin{bmatrix} d_1^2 & d_1 d_4 & d_1 d_5 \\ d_1 d_4 & d_2^2 + d_4^2 & d_4 d_5 + d_2 d_6 \\ d_1 d_5 & d_4 d_5 + d_2 d_6 & d_3^2 + d_5^2 + d_6^2 \end{bmatrix} \tag{11}$$

Thus, the posterior probability distribution of $\boldsymbol{d} = \{d_j, \alpha | j = 1:6\}$ can be calculated using Eq. (12).

$$P(\boldsymbol{d}|\boldsymbol{r}) \propto P_7(\alpha) P(\boldsymbol{r}|\boldsymbol{d}) \prod_{j=1}^{6} P_j(d_j) \tag{12}$$

The Bayesian model provided, written in OpenBUGS [33,37] code, is shown in Table 1 for the logistic case.

In the Bayesian model shown in Table 1, a uniform probability distribution between 0.01 and 2 is supposed for the d_j priors. This assumption is based on prior knowledge about the g_j coefficients in used CIE94 color-difference formula. Under this assumption and considering Eqs. (10,11), coefficients may vary among the values shown in Table 2.

According to Table 2, the allowed range for the variation of the g_j coefficients include those coefficients obtained when using CIE94 color-difference formula because with this formula the principal semi-axes of the ellipsoid are greater than or equal to 1 and then, when rotated, the coefficients g_1, g_2, and g_3 can't be greater than the squared inverses of the principal semi-axes of the ellipsoid. Therefore, the mentioned coefficients should be less than or equal to unity. Moreover, it is not difficult to show that absolute values of the g_4, g_5, and g_6 coefficients of a rotated ellipsoid should be less than or equal to half of the mentioned g_1, g_2, and g_3 upper limit. So, in our CIE94 case their absolute value should be less than or equal to 0.5. Nevertheless, wider ranges can be adopted for lower-informative priors of d_j if suspected that g_j coefficients could be outside the initial range. Usually, if convergence is achieved, posterior distribution of parameters should be very little affected by the selection of lower-informative priors. In any case, it would be easy to detect that the initial hypothesis on the probability distributions priors of d_j coefficients are incorrect because the resulting posterior distribution would show truncations at the ends of the intervals and even convergence problems could arise.

A uniform probability distribution between 0.1 and 50 is assumed for α prior because the standard deviation of the logistics distribution is $\sigma = \pi/(\alpha\sqrt{3}) = 18.14$ if $\alpha = 0.1$. This allows the possibility that 30% of observers do not notice a color difference between two stimuli whose ΔE^*_{ab} color difference is over 18, which contradicts the observations. Moreover, α values greater than 50 imply very small standard deviations, e.g., $\sigma = \pi/(\alpha\sqrt{3}) = 0.03$ for $\alpha = 50$, meaning that the observers should have a color-difference resolution beyond the human color perception capabilities.

The proposed Bayesian model would provide the upper limit of the parameters of the color discrimination ellipsoid at threshold, since observers are required to indicate the first pair of patches in each strip in which they observe a just noticeable color difference (JND), assuming that in the previous pair of patches they do not observe color difference.

A procedure, similar to that proposed in [26], to directly estimate the values of the color discrimination ellipsoid parameters at threshold would be to map the recorded frequency values

Optics EXPRESS

Table 1. Implementation of proposed model in OpenBUGS code [33,37]

```
model;
{
d1 ~ dunif(0.01,2)
d2 ~ dunif(0.01,2)
d3 ~ dunif(0.01,2)
d4 ~ dunif(−2,2)
d5 ~ dunif(−2,2)
d6 ~ dunif(−2,2)
alfa ~ dunif(0.1,50)
g1 <- (d1*d1)
g2 <- (d2*d2) + (d4*d4)
g3 <- (d3*d3) + (d5*d5) + (d6*d6)
g4 <- (d1*d4)
g5 <- (d1*d5)
g6 <- (d4*d5) + (d2*d6)
S <- pi()/(alfa*sqrt(3))
for(i in 1:N) {
 r[i,1:K] ~ dmulti(p[i,1:K],nRep)
 for (k in 1:K) {
dX2[i,k] <- (g3*dL[i,k]*dL[i,k]) + (g1*dA[i,k]*dA[i,k])+(g2*dB[i,k]*dB[i,k])+
   ((2*g4)*dA[i,k]*dB[i,k])+((2*g5)*dA[i,k]*dL[i,k])+((2*g6)*dB[i,k]*dL[i,k])
 dX[i,k] <- sqrt(dX2[i,k])
 dy[i,k]<-exp(alfa*(1- dX[i,k]))
pd[i,k]<- (dy[i,k] /((1+dy[i,k])*(1+dy[i,k])))*alfa
 }
 sumpd[i] <- sum(pd[i,1:K])
 for (k in 1:K) {
 p[i,k] <- pd[i,k] / sumpd[i]
 }
 }
}
```

Table 2. Variation ranges of g_j and α coefficients when $d_1, d_2, d_3 \in [0.01,\ 2]$ and $d_4, d_5, d_6 \in [-2,\ 2]$.

Parameter	Relationship between g_j and d_j	Min.	Max.
g_1	${d_1}^2$	0.0001	4
g_2	${d_2}^2 + {d_4}^2$	0.0001	8
g_3	${d_3}^2 + {d_5}^2 + {d_6}^2$	0.0001	12
g_4	$d_1 * d_4$	−4	4
g_5	$d_1 * d_5$	−4	4
g_6	$d_4 * d_5 + d_2 * d_6$	−8	8
α	-	0.1	50

Optics EXPRESS

to the mean value of the color differences between one pair patch and the previous one, replacing values $\Delta L^*_{ik}, \Delta a^*_{ik}, \Delta b^*_{ik}$ given in Eq. (5) by the values $\overline{\Delta} L^*_{ik}, \overline{\Delta} a^*_{ik}, \overline{\Delta} b^*_{ik}$, calculated according to Eqs. (13)–(15).

$$\overline{\Delta} L^*_{ik}=(\Delta L^*_{ik}+\Delta L^*_{ik-1})/2,\ k = 1 \ldots K \tag{13}$$

$$\overline{\Delta} a^*_{ik}=(\Delta a^*_{ik}+\Delta a^*_{ik-1})/2,\ k = 1 \ldots K \tag{14}$$

$$\overline{\Delta} b^*_{ik}=(\Delta b^*_{ik}+\Delta b^*_{ik-1})/2,\ k = 1 \ldots K \tag{15}$$

Assuming $\Delta L^*_{i0} = 0, \Delta a^*_{i0} = 0, \Delta b^*_{i0} = 0$.

2.2. Bayesian model verification with respect to the same theoretical data simulated in [26]

To verify the behavior of the Bayesian model, indicated in section 2.1, we will first analyze the results from the theoretically generated frequency data for four *CIE* color centers [19] as indicated in section 2.5 of [26], that, in summary, consists of determining the probability of observing a color difference in each pair of patches in a strip from the psychometric (*Logistic*) curve and the selected color difference model (*CIE94*); with the calculated probability (p), frequency values are randomly generated in each pair of patches from a binomial distribution with probability p and N repetitions; then the first pair of patches whose observed frequency is greater than 50% and which is closest to the end of the strip with the smallest color difference is selected and assigned a value of 1 (0 for the rest of the pairs in the strip); repeating the process a number of times (usually 100) will give the observed frequency for every pair patches of been the *JND* pair in a strip.

Second, results will be analyzed from the frequency data generated by randomly introducing noise with respect to the color differences between pairs of patches in the strips, repeating the process described in the previous paragraph. The generated noise is applied to the color differences in the strip pairs by adding a random error $N(0, \sigma_{cd})$ of zero mean and standard deviation σ_{cd}.

2.3. Parametric effects due to the use of the Bayesian approach when applied to real data published in [28]

To verify the Bayesian model behavior with real data, the data obtained in [28] will be analyzed for the generated strip pairs, around *CIE* red color center. The strips were printed using an Epson SureColor P7000 inkjet printer on 250 g/m2 Epson Premium Semigloss Photo Paper. Three sets of 8 pairs of strips were printed according to the vector directions scheme shown in Fig. 1 of [28], which correspond to the set of directions defined in the a^*-b^* plane by the color center and the vertices and midpoints of the edges of a square whose center coincides with the color center. The first set of pairs corresponded with pairs of samples arranged on the strip without separation, the second with a separation by 0.5 mm thick black line and the third set with the color samples separated 3 mm on a white background. The strips were evaluated 10 times by 15 observers with normal color vision, according to the Farnsworth-Munsell test of 100 shades. The observers were asked to indicate the number of patches pair on each strip at which they began to perceive a just noticeable color difference (*JND*), so that only one frequency record was obtained per strip per observer's evaluation. During the evaluation, the strips were observed in a Verivide viewer equipped with a Master TL-D90 Graphica 18 W/965 lamp with a color temperature of 6500K and an index Ra=98 and a background color corresponding to a neutral gray with CIELAB coordinates $L^*=62$, $a^*=0$, $b^*=0$.

3. Results

The proposed model defined in Eqs. (3)–(12) was implemented in MATLAB, using the *slicesample* function to sample marginal posterior probability distribution of the parameters from Eq. (12).

Optics EXPRESS

The MATLAB function *slicesample* uses the slice sampling algorithm of Neal [38] to generate Markov Chain Monte Carlo (MCMC) samples.

3.1. Relative to the simulated data generated in [26]

The results of applying the proposed Bayesian Strip Comparison Method (BSCM) to the theorical data shown in Table 1 of [26] for CIE red color center are shown in Table 3.

Table 3. Results for CIE red (*L*=44, a*=37, b*=23*) color center using MATLAB *slicesample* function for theoretical data shown in Table 1 of [26], where *Sd* is standard deviation, *MC_error* is Monte Carlo error, and *2.5 pc* and *97.5 pc* are 2.5 and 97.5 percentiles, respectively. Sample indicates the number of chain samples that were considered to simulate posterior distributions. *Start* indicates the first sample considered after the burn-in period needed to obtain convergence of distribution. g_j are the estimated parameters of the ellipsoid and $S = \pi/(\alpha\sqrt{3})$ is the estimated standard deviation of the psychometric curve.

	Mean	Sd	Mc_error	2.5 pc	Median	97.5 pc	Start	Sample
g_1	0.1905	0.0029	0.0001	0.1845	0.1905	0.1961	1001	2000
g_2	0.2988	0.0035	0.0001	0.2920	0.2987	0.3060	1001	2000
g_3	1.0085	0.0080	0.0004	0.9917	1.0086	1.0243	1001	2000
g_4	−0.1111	0.0023	0.0001	−0.1157	−0.1111	−0.1067	1001	2000
g_5	−0.0001	0.0044	0.0002	−0.0087	0.0000	0.0082	1001	2000
g_6	−0.0022	0.0053	0.0003	−0.0125	−0.0021	0.0080	1001	2000
S	0.1304	0.0024	0.0002	0.1260	0.1305	0.1350	1001	2000

Convergence behavior is shown in Fig. 2 after the burn-in period of 1000 iterations. A kernel of the marginal posterior probability distribution of the parameters is shown in Fig. 3. No truncation observed in the posterior probability distributions allows as concluding that hypothesis made about the prior probability distributions assumed in Table 2 were correct. Similar results were observed for other CIE color centers shown in the Table 4.

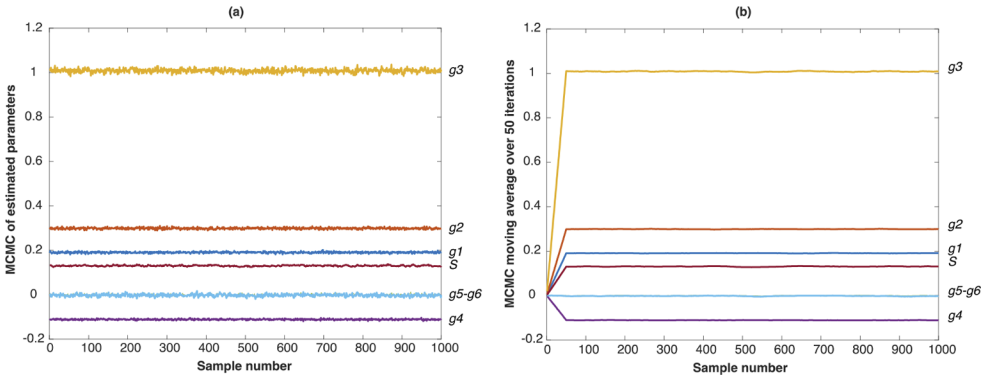

Fig. 2. Trace plots of simulated MCMC (a) and corresponding moving average over 50 iterations (b) from posterior probability distribution of g_j parameters after a burn-in period of 1000 iterations.

Table 4 compares the results between BSCM, SCM [26] and CIE94 ellipsoids for shown CIE color centers. The θ values obtained by SCM and by BSCM for the CIE gray color center are not included in Table 4 because the CIE94 color discrimination ellipsoids of the CIE gray color center degenerate into a sphere and, therefore, small differences in the size of one of its major axes generate large differences in the orientation of its major axis, leading to a large scatter of the θ values obtained.

Optics EXPRESS

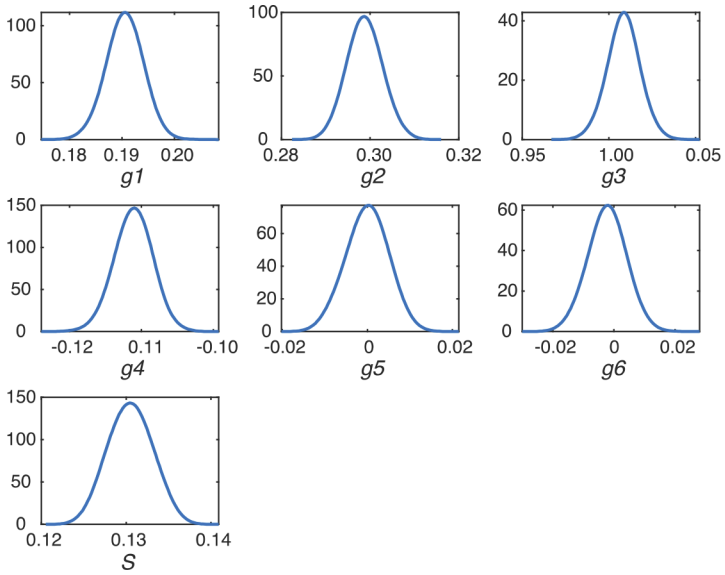

Fig. 3. Kernel plots of estimated marginal posterior density probability distributions of model parameters.

As shown in Table 4, the ellipsoid parameters using BSCM fit quite well the CIE 94 ellipsoids of the underlying model and the parameters estimated using SCM [26]. The results have been obtained by applying SCM and BSCM over randomly generated frequency data, repeating 50 times the procedure indicated in section 2.2.

The effect from the application of an error $N(0, \sigma_{cd})$ on the simulated theoretical color differences, as described in section 2.2, on the main parameters of color discrimination ellipsoids predicted by BSCM, are shown in Figs. 4 and 5.

As can be seen, the results shown in Figs. 4 and 5 are similar to those shown in Figs. 3–5 of [26]. A summary of the mean values obtained are shown in Table 5, where K is the factor size, calculated as the cubic root of the ellipsoid volume, $K = (4/3\pi abc)^{1/3}$.

To compare the results quantitatively, the evolution of the shape factors for SCM and BSCM relative to the shape factors of the CIE ellipsoids of the underlying model are shown in Table 6. Mean values evolution of the relative factor size for all four-color centers are shown in last rows of Table 6. As can be seen, the size of the estimated ellipsoids tends to be reduced for both methods as the noise introduced in the value of the color differences of the pairs of patches in the strips increases, but by BSCM the reduction is smaller than by SCM. It also can be observed from Table 5 that there are no bias of the predicted parameters by BSCM for $\sigma_{cd} = 0.2$, which is, approximately, the expected precision reachable when printing samples carefully using today's digital printing systems, as reported in [26].

On average, there is no bias for the parameters estimated by BSCM for $\sigma_{cd} = 0 \div 0.2$ and about -2% for $\sigma_{cd} = 0.3$, very similar to the bias of the parameters estimated by SCM [26], which ranges from about $+1\%$ for $\sigma_{cd} = 0$ to about -3% for $\sigma_{cd} = 0.3$.

3.2. Relative to the real data generated in [28]

Table 7 shows the results of applying the proposed BSCM to the real data reported in [28] for the three cases analyzed, where s_0 refers to the case of samples in contact, without separation, b_{05} refers to the case of pairs of samples separated by a 0.5 mm thick black line and w_3 to pairs of samples separated 3 mm on a white background. The results shown in Table 5 of this paper are

Optics EXPRESS

Table 4. Comparison between the results obtained by BSCM, SCM [26] and CIE94 ellipsoids of the assumed theoretical model to generate data for specified CIE color centers.

Cc [L* a* b*]	Model	g_1	g_2	g_3	g_4	g_5	g_6	a	b	c	θ	S
Red [44 36 22]	CIE94	0.1842	0.2956	1.0000	−0.1128	0.0000	0.0000	2.96	1.65	1.00	31.87	0.11
	SCM	0.1960	0.3164	1.0731	−0.1202	−0.0025	0.0030	2.90	1.64	0.99	31.81	-
	2σ	0.014	0.022	0.0702	0.0136	0.047	0.05	0.14	0.06	0.03	0.31	-
	BSCM	0.1822	0.2893	0.9666	−0.1101	−0.0008	−0.0012	2.97	1.67	1.02	32.04	0.12
	2σ	0.0052	0.0075	0.0163	0.0038	0.0066	0.0095	0.05	0.02	0.01	1.10	0.01
Yellow [87 −7 47]	CIE94	0.3357	0.1067	1.0000	0.0349	0.0000	0.0000	3.14	1.71	1.00	98.47	0.11
	SCM	0.3430	0.1111	1.0193	0.0355	0.0002	0.0000	3.08	1.69	0.99	98.52	-
	2σ	0.0025	0.0010	0.0048	0.0013	0.0032	0.0028	0.01	0.01	0.002	0.29	-
	BSCM	0.3270	0.1061	0.9927	0.0331	0.0011	−0.0011	3.14	1.74	1.00	98.33	0.13
	2σ	0.0076	0.0032	0.0166	0.0052	0.0139	0.0079	0.06	0.02	0.01	1.10	0.01
Green [56 −32 0]	CIE94	0.1681	0.4567	1.0000	0.0000	0.0000	0.0000	2.44	1.48	1.00	180	0.11
	SCM	0.1730	0.4646	1.0176	0.0002	0.0000	0.0000	2.40	1.47	0.99	180	-
	2σ	0.0014	0.0028	0.049	0.0021	0.0030	0.031	0.01	0.01	0.002	0.4	-
	BSCM	0.1648	0.4553	0.9834	0.0004	−0.0028	0.0108	2.46	1.48	1.01	180	0.13
	2σ	0.051	0.0113	0.0139	0.0054	0.0070	0.0117	0.04	0.02	0.01	1.06	0.01
Blue [35 5−31]	CIE94	0.4548	0.1791	1.0000	0.0457	0.0000	0.0000	2.37	1.46	1.00	279	0.11
	SCM	0.4605	0.1851	0.9961	0.0633	0.0004	0.0006	2.42	1.45	1.00	282	-
	2σ	0.0033	0.0018	0.0053	0.0022	0.0034	0.0035	0.01	0.01	0.01	0.43	-
	BSCM	0.4490	0.1765	0.9822	0.0374	0.0009	−0.0007	2.42	1.48	1.01	278	0.13
	2σ	0.0123	0.0060	0.0207	0.0064	0.0094	0.0079	0.04	0.02	0.01	1.28	0.01
Gray [62 0 0]	CIE94	1.0000	1.0000	1.0000	0.0000	0.0000	0.0000	1.00	1.00	1.00	0	0.11
	SCM	1.0334	1.0328	1.0336	0.0007	−0.0002	−0.0002	0.99	0.98	0.98	-	-
	2σ	0.0078	0.0086	0.0083	0.0069	0.0047	0.0058	0.01	0.01	0.01	-	-
	BSCM	1.0769	1.0523	1.0757	−0.0008	−0.0221	0.0083	0.98	0.97	0.96	-	0.13
	2σ	0.0418	0.0448	0.0425	0.0220	0.0216	0.0226	0.02	0.02	0.02	-	0.01

the same as those shown in Table 5 of [28] except for those concerning BSCM. Table 5 of [28] showed the results of applying the Bayesian model specified by Eqs. (1)–(12), without including the correction indicated in Eqs. (13)–(15), while Table 7 does show the parameters obtained including the mentioned correction. Because of this, the parameters specified in Table 7 are smaller than those indicated in Table 5 of [28], since if we do not apply the correction indicated in Eqs. (13)–(15) we would obtain the upper limit of the chromatic discrimination ellipse at the threshold.

In Table 7, as in Table 5 of [28], the results by SCM are compared to the results by PCM, after trimming the patch pairs from the strips.

For both PCM and SCM, the Bayesian method and T50 were applied. The Bayesian method for PCM corresponds with that described by Brusola et al. [30] and that described in this paper for SCM. T50 method for PCM and SCM corresponds to the fitting technique described by Melgosa et al. [39], as indicated in [28]. The resulting chromatic discrimination ellipses are shown in Fig. 6.

As already described in [28] the resulting chromatic discrimination ellipses by T50 and by the Bayesian technique are quite similar when applied to PCM or SCM, appreciating a clear parametric effect due to applying SCM, whereby the ellipses obtained by SCM are slightly larger

Optics EXPRESS

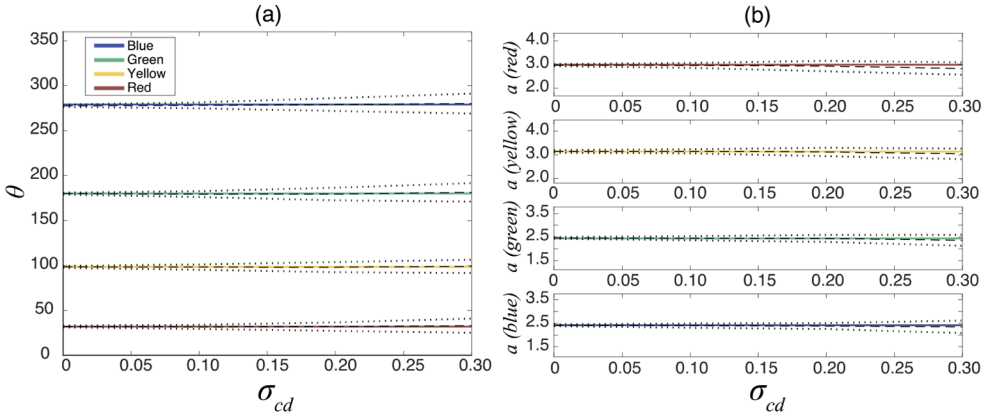

Fig. 4. Evolution of $\boldsymbol{\theta}$ and major axis, $\boldsymbol{a}$, from color discrimination ellipsoids of the specified CIE color centers as a function of σ_{cd}. Continuous lines correspond to the true values of the simulated model, dashed lines correspond to the mean values of the estimated parameters obtained by BSCM for 50 sets of samples, generated randomly, adding an error $N(0, \sigma_{cd})$ to the theoretical color differences. Dotted lines correspond to the 2.5 and 97.5 percentiles of the posterior distribution of the mean of the estimated parameter.

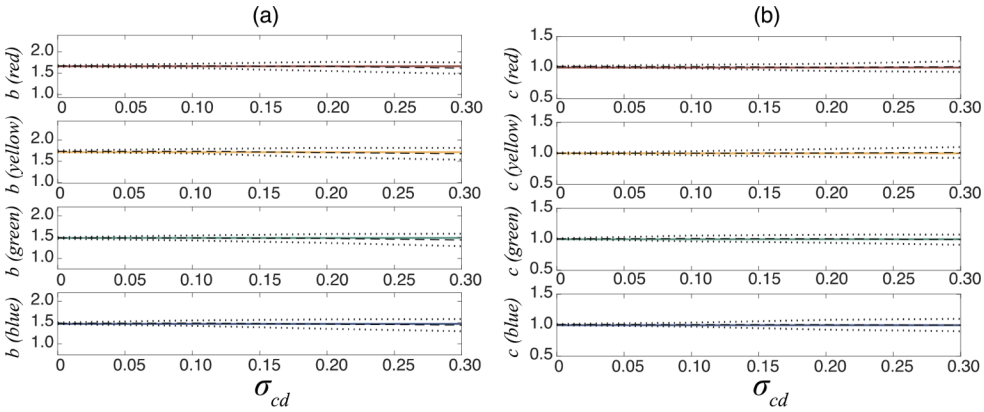

Fig. 5. Evolution of the intermediate axis, b, and minor axis, c, from color discrimination ellipsoids of the specified CIE color centers as a function of σ_{cd}. Continuous lines correspond to the true values of the simulated model, dashed lines correspond to the mean values of the estimated parameters obtained by BSCM for 50 sets of samples generated randomly, adding an error $N(0, \sigma_{cd})$ to the theoretical color differences. Dotted lines correspond to the 2.5 and 97.5 percentiles of the posterior distribution of the mean of the estimated parameter.

Optics EXPRESS

Table 5. Mean values of the parameters shown in Figs. 4 and5 and the CIE gray color center obtained by BSCM and the corresponding CIE94 parameters of the underlaying model used to simulate data.

Color Center	Parameter	σ_{cd}				CIE 94
		0	0.1	0.2	0.3	
Red	θ	32.03	31.58	31.89	32.91	31.87
	a	2.97	2.96	2.93	2.83	2.96
	b	1.67	1.67	1.66	1.62	1.65
	c	1.02	1.01	1.00	1.01	1.00
	K	2.77	2.76	2.73	2.69	2.73
	S	0.12	0.12	0.13	0.15	0.11
Yellow	θ	98	98	98	99	98
	a	3.14	3.15	3.12	3.04	3.14
	b	1.74	1.74	1.70	1.67	1.71
	c	1.00	1.00	1.01	1.01	1.00
	K	2.84	2.84	2.82	2.79	2.82
	S	0.13	0.13	0.13	0.15	0.11
Green	θ	180	179	179	181	180
	a	2.46	2.45	2.44	2.36	2.44
	b	1.48	1.48	1.47	1.43	1.48
	c	1.01	1.01	1.01	0.99	1.00
	K	2.49	2.49	2.47	2.42	2.47
	S	0.13	0.13	0.14	0.15	0.11
Blue	θ	278	278	279	280	279
	a	2.42	2.40	2.38	2.35	2.37
	b	1.48	1.49	1.47	1.44	1.45
	c	1.01	1.01	1.01	0.99	1.00
	K	2.47	2.47	2.45	2.41	2.43
	S	0.13	0.13	0.14	0.15	0.11
Gray [a]	a	0.98	1.04	1.08	1.11	1.00
	b	0.97	0.97	0.98	0.97	1.00
	c	0.96	0.93	0.90	0.86	1.00
	K	1.56	1.58	1.59	1.57	1.61
	S	0.12	0.12	0.13	0.17	0.11

[a] θ values for the CIE gray color center are not included (see third paragraph of section 3.1).

Optics EXPRESS

Table 6. Relative factor size of the discrimination ellipsoids computed by SCM and BSCM with respect to factor size of CIE94 discrimination ellipsoids of the underlaying model used to simulate data. The size factor shown in this table correspond to the size factor *K* divided by the factor size of the corresponding CIE94 ellipsoid.

Color Center	Par	σ_{cd} 0	0.1	0.2	0.3	CIE 94	Color Center	Par	σ_{cd} 0	0.1	0.2	0.3	CIE 94
Red	BSCM	1.01	1.01	1.00	0.98	1.00	Blue	BSCM	1.02	1.02	1.01	0.99	1.00
	2σ	0.02	0.06	0.13	0.17			2σ	0.03	0.08	0.14	0.21	
	SCM	1.01	1.00	0.99	0.97			SCM	1.02	1.01	0.99	0.97	
	2σ	0.01	0.08	0.17	0.27			2σ	0.01	0.08	0.16	0.24	
Yellow	BSCM	1.01	1.01	1.00	0.99	1.00	Gray	BSCM	0.97	0.98	0.98	0.97	1.00
	2σ	0.03	0.06	0.12	0.16			2σ	0.02	0.06	0.10	0.17	
	SCM	1.01	1.00	0.99	0.97			SCM	0.98	1,00	0.97	0.96	
	2σ	0.01	0.07	0.14	0.23			2σ	0.01	0.05	0.09	0.12	
Green	BSCM	1.01	1.01	1.00	0.98	1.00	Mean	BSCM	1.00	1.00	1.00	0.98	1.00
	2σ	0.02	0.08	0.13	0.18			2σ	0.02	0.07	0.12	0.18	
	SCM	1.01	1.00	0.98	0.96			SCM	1.01	1.00	0.98	0.97	
	2σ	0.01	0.07	0.16	0.24			2σ	0.01	0.07	0.14	0.22	

Table 7. Chromaticity discrimination ellipse parameters in Δ*a-Δ*b** plane.[a]**

Case	Method	Fitting	*g11*	*g22*	*g12*	*A*	*B*	*θ*	*Tilt*	*KG*	*S*	*2σ*
s0	PCM	Bayesian	1.34	0.91	−0.22	1.11	0.84	68°	36°	1.71	0.71	8°
		T50	1.19	0.84	−0.20	1.16	0.88	66°	34°	1.79	-	-
	SCM	Bayesian	0.89	0.52	0.07	1.42	1.05	100°	68°	2.16	0.43	9°
		T50	0.78	0.49	0.05	1.44	1.13	99°	67°	2.26	-	-
b05	PCM	Bayesian	1.70	1.38	−0.46	0.98	0.70	54°	22°	1.47	0.92	6°
		T50	1.69	1.02	−0.33	1.06	0.74	68°	36°	1.57	-	-
	SCM	Bayesian	0.91	0.75	−0.25	1.33	0.96	54°	22°	2.00	0.7	9°
		T50	0.67	0.56	−0.10	1.40	1.17	59°	27°	2.27	-	-
w3	PCM	Bayesian	1.14	0.92	−0.25	1.15	0.88	57°	25°	1.78	1.36	8°
		T50	0.90	0.81	−0.17	1.21	0.99	53°	21°	1.94	-	-
	SCM	Bayesian	0.52	0.56	−0.10	1.52	1.25	40°	8°	2.44	0.63	14°
		T50	0.45	0.42	−0.05	1.61	1.43	55°	23°	2.69	-	-

[a] g_{11}, g_{22}, and g_{12}: metric coefficients of the ellipse ($g_{11=}\ g_1$, $g_{22=}\ g_2$, $g_{12=}\ g_4$ from 2D version of Eq. (5)); A and B: major and minor semi-axes, respectively; θ: angle of the major axis with respect to $+a^*$; *Tilt* ($\Delta\theta$): angular difference between the hue angle (h^*_{ab}) of the color center and the angle of the major axis of the discrimination ellipses with respect to $+a^*$, in this order; K_G: size factor = $\sqrt{\pi AB}$; S: standard deviation of the psychometric curve; 2σ: twice the standard deviation of the posterior distribution of θ (equivalent to a credibility interval of 95% probability); s_0: samples with no separation; b_{05}: samples separated by a black line 0.5 mm thick; w_3: samples separated 3 mm on white background.

Optics EXPRESS

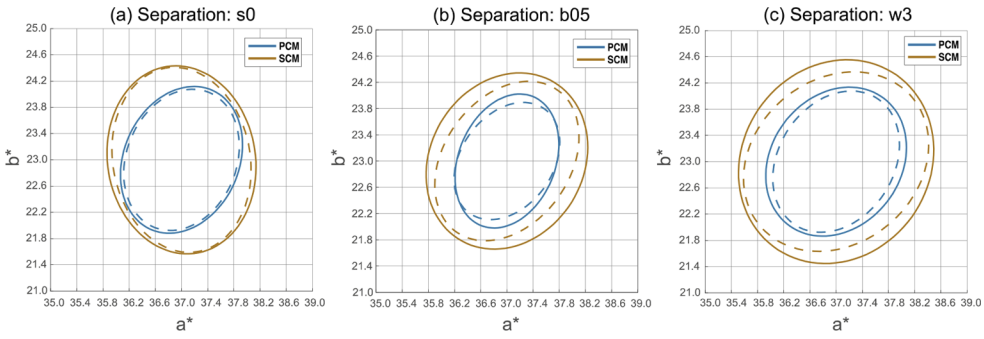

Fig. 6. Plot of the Chromaticity-discrimination ellipses at threshold shown in Table 5. Continuous lines correspond to chromaticity discrimination ellipses obtained by T50 method and dashed lines correspond to chromaticity discrimination ellipses obtained by Bayesian methods. The ellipses shown obtained by BSCM (dashed line of SCM) do not coincide with those shown in Fig. 7 of [28] because those shown in [28] were calculated not applying the correction indicated in Eqs (13)–(15), so that they correspond to the upper limit of the chromatic discrimination ellipses, not with the estimated value at threshold.

than those obtained by PCM. Although, the size factors reported by Huang et al. [16] and Xu et al. [29], using PCM, are much closer to those obtained by SCM.

We refer the interested reader to the results section in [28] about the parametric effect observed on the chromatic discrimination ellipses when applying SCM to the different cases exposed.

As can be seen in Fig. 6, the chromatic discrimination ellipses estimated by the Bayesian approach are slightly smaller than those obtained by PCM and SCM. In contrast to that shown in Fig. 7 of [28] in which the ellipses obtained by BSCM are slightly larger than those obtained by SCM, using the T50 fitting method.

With the parameters estimated by BSCM, with the correction indicated in Eqs. (13)–(15), the same degree of regularity reported in [28] is observed between the tilt of the ellipses obtained by PCM, BPCM (Bayesian Pair Comparison Method), SCM and BSCM for pairs of patches separated by a 0.5 mm thick black line and for patches separated 3 mm on a white background, and a large discrepancy of the tilt between PCM and SCM for pairs of patches with no separation. So, parametric effect on the tilt due to SCM is confirmed for no separation patches case.

Again, as in [28], Table 7 shows a similar reduction in S, standard deviation of the psychometric curve, of BSCM relative to BPCM, suggesting some reduction in the degree of observer confusion when performing color difference tests at threshold by SCM.

4. Discussion

In this paper a Bayesian alternative to the SCM method reported in [26] has been proposed. The application of the Bayesian model to the same simulated theoretical data used in [26] indicates a high degree of agreement between the parameters estimated by both methods, either under ideal conditions, without the presence of noise, or with the presence of simulated noise, by adding to the theoretical color differences of the color samples a random error of probability distribution $N(0, \sigma_{cd})$. As σ_{cd} increases with respect to the simulated data, the results obtained indicate that, as by SCM, the size factor of the estimated color difference ellipsoids decreases with respect to the size factor of the underlying model in the simulation (corresponding to CIE94 ellipsoids of the CIE color centers shown in [26] and frequency data generated from the logistic curve with parameters $\alpha = \beta = 2$). However, by BSCM, the size factor is reduced less than by SCM, the variation being about 2% by BSCM and about 3% by SCM for $\sigma_{cd} = 0.3$. Both methods

Optics EXPRESS

show a slight bias for data without noise ($\sigma_{cd} = 0$), but this bias disappears for $\sigma_{cd} = 0.2$, which corresponds to the noise expected if carefully printed with current printing systems.

On the other hand, the Bayesian method allows to estimate the sigma (S) of the psychometric curve of the underlying model, which is not possible directly by SCM. The results show that the values of S estimated by the Bayesian model agree quite approximately with the expected value, according to the median theorem, although they also show a tendency to increase as the presence of noise increases.

The results obtained by applying the proposed Bayesian model to the same real data reported in [28] indicate small differences between the parameters estimated by both methods. By BSCM a slight tendency to reduce the factor size K_G is appreciated, in the same way as it occurs when using BPCM in relation to PCM. Regarding the tilt of the chromatic discrimination ellipses, the difference of the estimated values between BSCM and SCM are always within the range of the 95% credibility interval of the parameter estimated by BSCM, which with the real data range from 8° to 14° as shown in Table 7.

Given data, the main advantage of using the Bayesian method over the non-Bayesian version is that the Bayesian method allows a direct analysis of the precision or statistical variability of the estimated parameters, or any function dependent on them, from the corresponding credibility intervals or any other measure of dispersion calculable from the resulting MCMC.

In addition, another advantage of BSCM is that it does not require the vectorization process, necessary for conventional SCM with real data, so that color differences of the pair patches in every strip are fitted to a vector direction through the origin. The results presented in this work have been obtained without applying any vectorization, so the BSCM results do not reflect any influence due to the mentioned preprocessing.

A minor drawback of BSCM, as is often the case with Bayesian methods, is the computational time. Processing times vary slightly around 1.5 seconds per 100 updates when the model is run using MATLAB (version R2019a, 64-bit application) on a MacBook Pro computer (64-bit, Intel Core i5 dual-core 3.1 GHz, 8 GB ram), yielding a total processing time of 30 seconds for the generation of 2000 samples, as is the case shown in Table 3, which can be considered negligible compared to the time spent on other necessary tasks when collecting color difference data.

Disclosures. The authors declare no conflicts of interest.

Data availability. Data underlying the results presented in this paper are not publicly available at this time but may be obtained from the authors upon reasonable request.

References

1. M. R. Luo, G. Cui, and B. Rigg, "BFD (l:c) colour difference formula Part 2 – Performance of the formula," J. Soc. Dyers Colour. **103**(3), 126–132 (2008).
2. M. R. Luo and B. Rigg, "BFD (l:c) colour difference formula Part 1 – Development of the formula," J. Soc. Dyers Colour. **103**(2), 86–94 (2008).
3. R. S. Berns, D. H. Alman, L. Reniff, G. D. Snyder, and M. R. Balonon-Rosen, "Visual determination of suprathreshold color-difference tolerances using probit analysis," Color Res. Appl. **16**(5), 297–316 (1991).
4. D.H. Kim and J. H. Nobbs, "New weighting functions for the weighted CIELAB colour difference formula," in *Proceedings of the AIC* (1997), pp. 446–449.
5. K. Witt, "Geometric relations between scales of small colour differences," Color Res. Appl. **24**(2), 78–92 (1999).
6. CIE No. 116, *Industrial Colour-Difference Evaluation* (Commission Internationale de l'Éclairage, 1995).
7. ISO/CIE No. 11664-6:2014, *Colorimetry – Part 6: CIEDE2000 colour-difference formula* (ISO, 2014).
8. M. R. Luo, G. Cui, and C. Li, "Uniform colour spaces based on CIECAM02 colour appearance model," Color Res. Appl. **31**(4), 320–330 (2006).
9. C. Li, Z. Li, Z. Wang, Y. Xu, M. R. Luo, G. Cui, M. Melgosa, M. H. Brill, and M. Pointer, "Comprehensive color solutions: CAM16, CAT16, and CAM16-UCS," Color Res. Appl. **42**(6), 703–718 (2017).
10. S.Y. Zhu, M. R. Luo, and G. Cui, "New experimental data for investigating uniform colour spaces," in *Proceedings of the 9th Congress of the International Colour Association* (AIC Color: Rochester, New York 2001), pp. 626–629.
11. D. L. MacAdam, "Uniform color scales," J. Opt. Soc. Am. **64**(12), 1691–1702 (1974).
12. S. S. Guan and M. R. Luo, "A colour-difference formula for assessing large colour differences," Color Res. Appl. **24**(5), 344–355 (1999).
13. S. Badu, Large colour differences between surface colours, PhD thesis, University of Bradford (1986).

Optics EXPRESS

14. M. R. Pointer and G. G. Attridge, "Some aspects of the visual scaling of large colour differences," Color Res. Appl. **22**(5), 298–307 (1997).
15. S. M. Newhall, "Preliminary report of the O.S.A. Subcommittee on the spacing of the Munsell colors," J. Opt. Soc. Am. **30**(12), 617–645 (1940).
16. M. Huang, H. Liu, G. Cui, M. R. Luo, and M. Melgosa, "Evaluation of threshold color differences using printed samples," J. Opt. Soc. Am. A **29**(6), 883–891 (2012).
17. M. Huang, H. Liu, G. Cui, and M.R. Luo, "Testing uniform colour spaces and colour-difference formulae using printed samples," Color Res. Appl. **37**(5), 326–335 (2012).
18. Q. Xu, B. Zhao, G. Cui, and M. R. Luo, "Testing uniform colour spaces using colour differences of a wide colour gamut," Opt. Express **29**(5), 7788–7793 (2021).
19. A. R. Robertson, "CIE guidelines for coordinated research on colour-difference evaluation," Color Res. Appl. **3**(3), 149–151 (1978).
20. M. Melgosa, "Request for existing experimental datasets on color differences," Color Res. Appl. **32**(2), 159 (2007).
21. K. Witt, "CIE guidelines for coordinated future work on industrial color-difference evaluation," Color Res. Appl. **20**(6), 399–403 (1995).
22. M. R. Luo and B. Rigg, "Chromaticity-discrimination ellipses for surface colours," Color Res. Appl. **11**(1), 25–42 (1986).
23. H. Wang, G. Cui, M. R. Luo, and H. Xu, "Evaluation of colour-difference formulae for different colour-difference magnitudes," Color Res. Appl. **37**(5), 316–325 (2012).
24. R. M. Rich, F. W. Billmayer, and W. G. Howe, "Method for deriving color-difference-perceptibility ellipses for surface- color samples," J. Opt. Soc. Am. **65**(8), 956–959 (1975).
25. R. M. Rich and F. W. Billmayer, "Small and moderate color differences," Color Res. Appl. **8**(1), 31–39 (1983).
26. F. Brusola, I. Tortajada, I. Lengua, B. Jordá, and G. Peris-Fajarnés, "Strip-pair comparison method for building threshold color-difference models: theoretical model validation," Opt. Express **28**(14), 21336–21347 (2020).
27. W.S. Torgerson, *Theory and Methods of Scaling* (John Wiley & Sons, 1958), Chap. 7.
28. F. Brusola, I. Tortajada, I. Lengua, B. Jordá, and G. Peris-Fajarnés, "Parametric effects by using the strip-pair comparison method around red CIE color center," Opt. Express **28**(14), 19966–19977 (2020).
29. H. Xu and H. Yaguchi, "Visual evaluation at scale of threshold to suprathreshold color difference," Color Res. Appl. **30**(3), 198–208 (2005).
30. F. Brusola, I. Tortajada, I. Lengua, B. Jordá, and G. Peris, "Bayesian approach to color-difference models based on threshold and constant-stimuli methods," Opt. Express **23**(12), 15290–15309 (2015).
31. K. Witt and G. Döring, "Parametric variations in a threshold color-difference ellipsoid for green painted samples," Color Res. Appl. **8**(3), 153–163 (1983).
32. A. Blasco, *Bayesian Data Analysis for Animal Scientists* (Springer, 2017).
33. I. Ntzoufras, *Bayesian Modeling Using WinBUGS* (John Wiley & Sons, 2009).
34. R. L. Wasserstein, A. L. Schirm, and N. A. Lazar, "Moving to a World Beyond p < 0.05," The American Statistician **73**(sup1), 1–19 (2019).
35. J. Orloff and J. Bloom, *Comparison of frequentist and Bayesian inference* (MIT OpenCourseWare, 2014), class 20 of 18.05 - Introduction to Probability and Statistics.
36. V. E. Johnson, "Revised standards for statistical evidence," PNAS **110**(48), 19313–19317 (2013).
37. OpenBUGS license, release (3.2.3). http://www.openbugs.net/ (Accessed 2021 Apr 18).
38. R. Neal, "Slice sampling," Ann. Statist. **31**(3), 705–767 (2003).
39. M. Melgosa, E. Hita, A. J. Poza, D. H. Alman, and R. S. Berns, "Suprathreshold color-difference ellipsoids for surface colors," Color Res. Appl. **22**(3), 148–155 (1997).